Ferromagnetic and Spin-Glass Finite-Temperature Order but no Antiferromagnetic Order in the d=1 Ising Model with Long-Range Power-Law Interactions

E. Can Artun[1,2] and A. Nihat Berker[2,3]

[1] *TUBITAK Research Institute for Fundamental Sciences (TBAE), Gebze, Kocaeli 41470, Turkey*
[2] *Faculty of Engineering and Natural Sciences, Kadir Has University, Cibali, Istanbul 34083, Turkey*
[3] *Department of Physics, Massachusetts Institute of Technology, Cambridge, Massachusetts 02139, USA*

The $d = 1$ Ising ferromagnet and spin glass with long-range power-law interactions $J\,r^{-a}$ is studied for all interaction range exponents a by a renormalization-group transformation that simultaneously projects local ferromagnetism and antiferromagnetism. In the ferromagnetic case, $J > 0$, a finite-temperature ferromagnetic phase occurs for interaction range $0.74 < a < 2$. The second-order phase transition temperature monotonically decreases between these two limits. At $a = 2$, the phase transition becomes first order, also as predicted by rigorous results. For $a > 2$, the phase transition temperature discontinuously drops to zero and for $a > 2$ there is no ordered phase above zero temperature, also as predicted by rigorous results. At the other end, on approaching $a = 0.74$ from above, namely increasing the range of the interaction, the phase transition temperature diverges to infinity, meaning that, at all non-infinite temperatures, the system is ferromagnetically ordered. Thus, the equivalent-neighbor interactions regime is entered before ($a > 0$) the neighbors become equivalent, namely before the interactions become equal for all separations. The critical exponents $\alpha, \beta, \gamma, \delta, \eta, \nu$ are calculated, from a large recursion matrix, varying as a function of a. For the antiferromagnetic case, $J < 0$, all triplets of spins at all ranges have competing interactions and this highly frustrated system does not have an ordered phase. In the spin-glass system, where all couplings for all separations are randomly ferromagnetic or antiferromagnetic (with probability p), a finite-temperatures spin-glass phase is obtained in the absence of antiferromagnetic phase. A truly unusual phase diagram is obtained. In the spin-glass phase, the signature chaotic behavior under scale change occurs in a richer version than previously: In the long-range interaction of this system, the interactions at every separation become chaotic, yielding a piecewise chaotic interaction function.

I. ORDERING IN ONE DIMENSION: LONG-RANGE INTERACTIONS

Whereas systems with finite-range interactions do not order above zero temperature in one dimension, certain systems with long-range interactions do order.[1–5] The archetypical example are the Ising ferromagnetic models with power-law interactions, $J\,r^{-a}$. Also as seen below, for antiferromagnetic interactions, the system incorporates saturated frustration and spin-glass ordering without antiferromagnetic ordering, in the absence of quenched randomness.

The model that we study is defined by the Hamiltonian

$$-\beta\mathcal{H} = \sum_{r_1 \neq r_2} J\,|r_1 - r_2|^{-a} s_{r_1} s_{r_2} + H \sum_{r_1} s_{r_1} \qquad (1)$$

where $\beta = 1/k_B T$ is the inverse temperature, r_1 and r_2 designate the sites on the one-dimensional system, at each site r_i there is an Ising spin $s_{r_i} = \pm 1$, and the sums are over all sites in the system. For ferromagnetic and antiferromagnetic systems, the two-spin interactions J are $J = |J| > 0$ and $J = -|J| < 0$, respectively. For the spin-glass system, for each two spins at any range, their interaction is randomly ferromagnetic (with probability $1 - p$) or antiferromagnetic (with probability p). The second term in Eq. (1) is the magnetic-field H term.

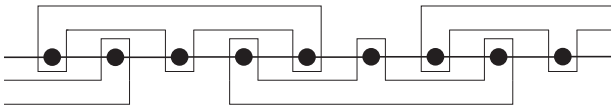

FIG. 1. Renormalization-group cells for $d = 1$. This cell structure projects both local ferromagnetism and antiferromagnetism, and therefore also spin-glass order.

II. METHOD: LONG-RANGE RENORMALIZATION GROUP

We solve this system with Niemeyer and van Leeuwen's two-cell cluster approximation.[6–8] The renormalization-group transformation is constructed by first choosing cells on the $d = 1$ system, as shown in Fig. 1. Each of our cells has three spins. This cell structure projects both local ferromagnetism and antiferromagnetism, and therefore also spin-glass order. Secondly, for each cell, a cell-spin is defined as the sign of the sum of the three spins in the cell,

$$s'_{r'} = signum(s_{r-2} + s_r + s_{r+2}) \qquad (2)$$

where the signum function returns the sign of its argument, primes denote the renormalized system, and $r' = r/b$, where $b = 3$ is the length-rescaling factor of the renormalization-group transformation. The renor-

malized interactions are obtained from the conservation of the partition function Z,

$$Z = \sum_{\{s\}} e^{-\beta\mathcal{H}(\{s\})} = \sum_{\{s'\}}\sum_{\{\sigma\}} e^{-\beta\mathcal{H}(\{s'\},\{\sigma\})} = \sum_{\{s'\}} e^{-\beta\mathcal{H}'(\{s'\})} = Z' , \quad (3)$$

where the summed variable σ represents, for each cell, the four states that give the same cell-spin value. Thus, the renormalized interactions are obtained from

$$e^{-\beta\mathcal{H}'(\{s'\})} = \sum_{\{\sigma\}} e^{-\beta\mathcal{H}(\{s'\},\{\sigma\})} . \quad (4)$$

The two-cell cluster approximation of Niemeyer and van Leeuwen consists in carrying out this transformation for two cells, including the 6 intracell interactions and the 9 intercell interactions. A recursion relation is obtained for each renormalized interaction,

$$J'_{r'} = \frac{1}{4}\ln\frac{R_{r'}(+1,+1)R_{r'}(-1,-1)}{R_{r'}(+1,-1)R_{r'}(-1,+1)} ,$$
$$H' = \frac{1}{4}\ln\frac{R_1(+1,+1)}{R_1(-1,-1)} , \quad (5)$$

where

$$R_{r'}(s'_0, s'_{r'}) = \sum_{\sigma_0,\sigma_{r'}} e^{-\beta\mathcal{H}_{0r'}} , \quad (6)$$

where the unrenormalized two-cell Hamiltonian contains the six intracell interactions and the 9 intercell interactions between the 6 spins in cells 0 and r'.

III. RESULTS: FINITE-TEMPERATURE FERROMAGNETIC PHASE IN $d = 1$

The calculated phase diagram of the $d = 1$ long-range ferromagnetic Ising model, with interactions $J\,r^{-a}$, is shown in Fig. 2, in terms of temperature $1/J$ and interaction range a. A finite-temperature second-order ferromagnetic phase transition occurs for $0.74 < a < 2$. The second-order phase transition temperature monotonically decreases between these two limits. At $a = 2$, phase transition becomes first order, as predicted by rigorous results [5] and also as seen from our calculated magnetization curves in Fig. 3. For $a > 2$ the phase transition temperature discontinuously drops to zero and there is no ordered phase above zero temperature, also as predicted by rigorous results [2, 3]. At the other end, on approaching $a = 0.74$ from above, the phase transition temperature diverges to infinity, meaning that, at all non-infinite temperatures, the system is ferromagnetically ordered. Thus, the equivalent-neighbor interactions regime is entered in fact before ($a > 0$) the neighbors become equivalent, namely before the interactions become equal for all separations. To the left of the dashed line on this figure is the equivalent-neighbor regime, where a strong-coupling phase transition, where the interactions are scaled with system size, is found .

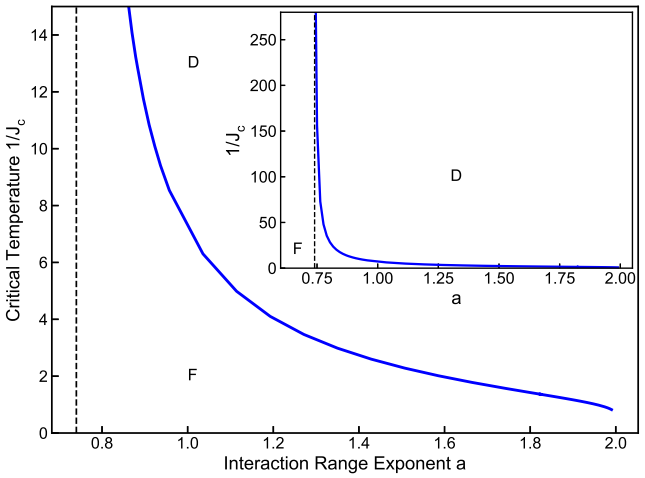

FIG. 2. Calculated phase diagram of the $d = 1$ long-range ferromagnetic Ising model with interactions $J\,r^{-a}$. Ferromagnetic (F) and disordered (D) phases are seen. A finite-temperature ferromagnetic phase transition occurs for $0.74 < a < 2$. The second-order phase transition temperature monotonically decreases between these two limits. At $a = 2$, the transition becomes first-order, as predicted by rigorous results [5] and also as seen from our calculated magnetization curves in Fig. 3 below. For $a > 2$ the phase transition temperature discontinuously drops to zero and there is no ordered phase above zero temperature, also as predicted by rigorous results [2, 3]. At the other end, on approaching $a = 0.74$ from above, the phase transition temperature diverges to infinity, meaning that, at all non-infinite temperatures, the system is ferromagnetically ordered. Thus, the equivalent-neighbor interactions regime is entered before ($a > 0$) the neighbors become equivalent, namely before the interactions become equal for all separations. To the left of the dashed line on this figure is the equivalent-neighbor regime, where a strong-coupling phase transition, where the interactions are scaled with system size, is found in Sec. V.

The calculated correlation-length critical exponent ν, correlation-function critical exponent η, specific heat critical exponent α, magnetization critical exponents β and δ, the susceptibility critical exponent γ, continuously varying as a function of interaction range a for the finite-temperature ferromagnetic phase transition, are shown in Fig. 4. These critical exponents are calculated, with $H = H' = 0$, from the relations $J'_1, ..., J'_n = \text{funct}(J_1, ..., J_n)$ of Eqs. (5,6). Convergence is obtained by calculation up to $n = 20$. The largest (and, as expected, only relevant, namely greater than 1) eigenvalue $\lambda_T = b^{y_T}$ of the derivative matrix of these recursion relations at the critical point gives the correlation-length critical exponent $\nu = 1/y_T$ and the specific heat critical exponent $\alpha = 2 - d/y_T = 2 - 1/y_T$. The magnetization critical exponents $\beta = (d - y_H)/y_T = (1 - y_H)/y_T$

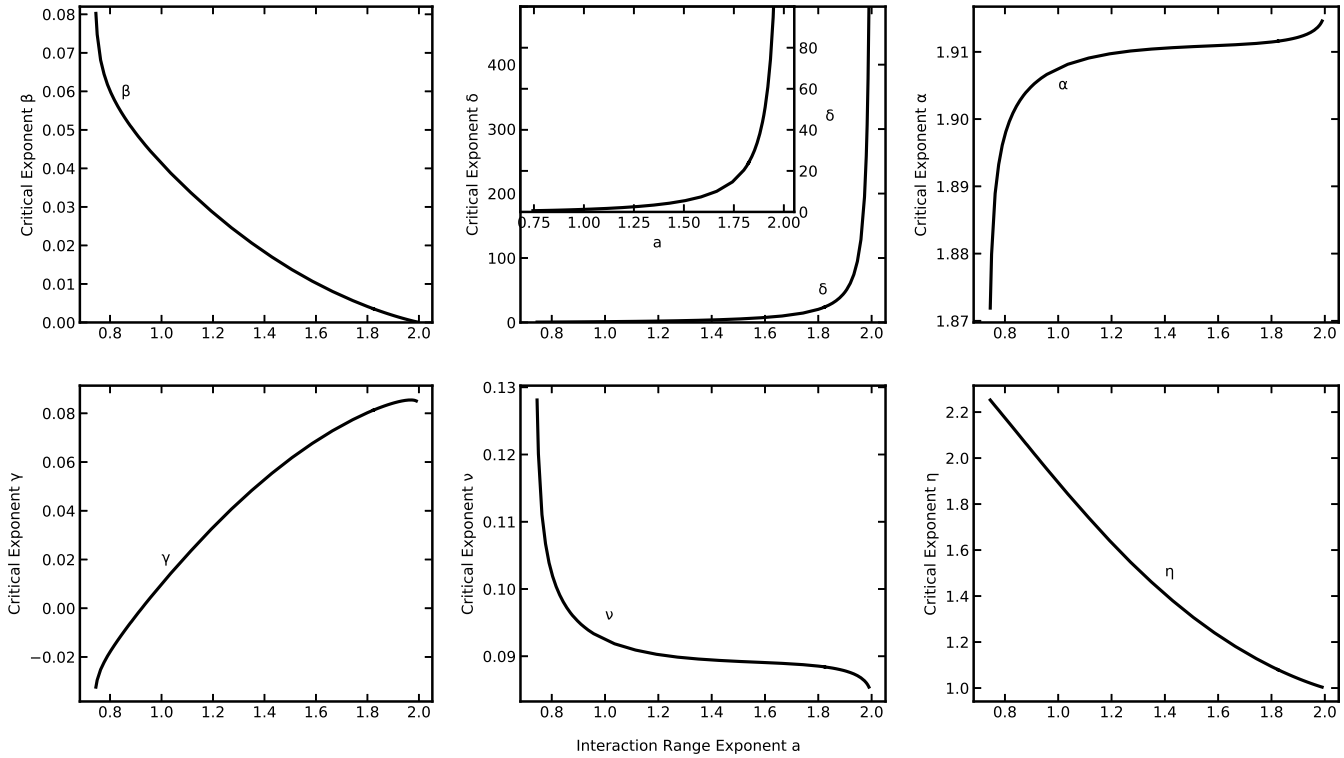

FIG. 3. Correlation-length critical exponent ν, correlation-function critical exponent η, specific heat critical exponent α, magnetization critical exponents β and δ, susceptibility critical exponent γ, as a function of interaction range a for the finite-temperature ferromagnetic phase transition. Note that β reaches 0 and δ diverges to infinity, as expected, as the first-order phase transition as $a = 2$ is reached from below.

and $\delta = y_H/(d - y_H) = y_H/(1 - y_H)$, the susceptibility critical exponent $\gamma = (2y_H - d)/y_T$, and the correlation-function critical exponent $\eta = 2 + d - y_H = 3 - y_H$ are calculated, at the critical point, with $H = H' = 0$, from $\partial H'/\partial H = b^{y_H}$.[8] Note that at $a = 2$, the magnetization critical exponent $\beta = 0$, which gives a first-order phase transition [9] as the temperature is scanned. At $a = 2$, the other magnetization critical exponent δ diverges to infitinity, which gives the first-transition as the magnetic field is scanned.

IV. CALCULATED MAGNETIZATION AND VARIABLE-RANGE ENERGY DENSITY CURVES: HYBRID-ORDER PHASE TRANSITION

Magnetization curves $M(T)$ are calculated by multiplying, along the renormalization-group trajectory, the magnetization recursion relation,

$$M_0 = b^{-n} M_n \cdot \left(\frac{\partial H'}{\partial H}\right)_n \cdots \left(\frac{\partial H'}{\partial H}\right)_2 \cdot \left(\frac{\partial H'}{\partial H}\right)_1, \qquad (7)$$

where the subscript n designates the nth renormalization-group transformation along the trajectory. Even when starting close to phase transition, the trajectory takes this product close to a phase-sink fixed point. At the disordered phase sink, $M_n = 0$, and thus at the starting temperature $M_0 = 0$. At the ferromagnetic ordered phase sink, $M_n = 1$ and $(\partial H'/\partial H)_n = b$, and thus at the starting non-zero temperature is calculated.

The thus calculated magnetization curves for the entire range of temperatures for each a are given in Fig. 4. For $0.74 < a < 2$, the magnetization curves show a second-order phase transition, with the magnetizations continuously reaching zero as the critical temperature is approached from below. The second-order phase transition temperature monotonically decreases between these two limits of a. At $a = 2$, the phase transition becomes first order, as seen by the large discontinuity in calculated magnetization only at $a = 2$. For $a > 2$ the phase transition temperature discontinuously drops to zero and there is no ordered phase above zero temperature, also as predicted by rigorous results [2, 3]. At the other end, on approaching $a = 0.74$ from above, the phase transition temperature diverges to infinity. For $a > 2$, the calculated magnetization is non-zero at all non-infinite temperatures as seen Fig. 3, and the system is ferromagnetically ordered. Thus, the equivalent-neighbor interactions regime is entered in fact before ($a > 0$) the neighbors become equivalent, namely before the interactions become equal for all separations. To the left of the dashed line on this figure is the equivalent-neighbor

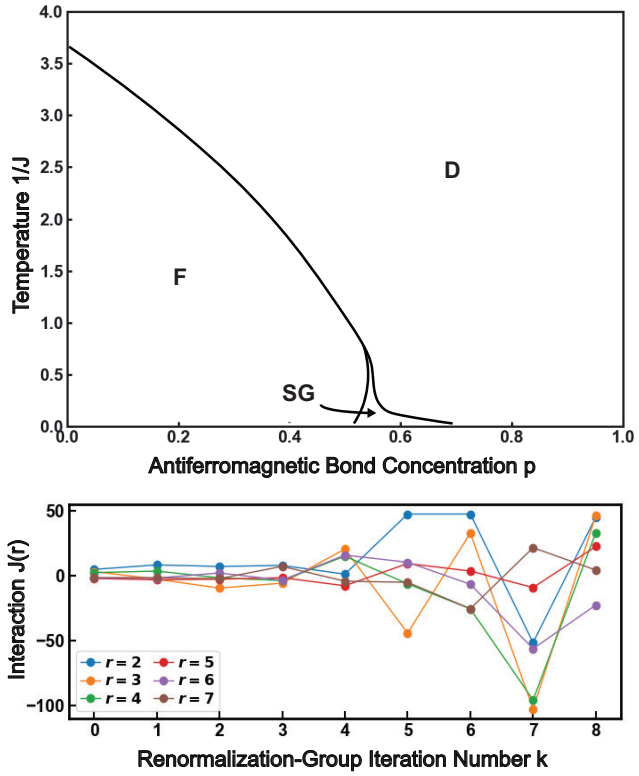

FIG. 4. Calculated finite-temperature phase diagram of the $d = 1$ long-range Ising spin-glass system with interaction-range exponent $a = 1$, where all couplings for all separations are randomly ferromagnetic or antiferromagnetic (with probability p). Ferromagnetic (F), spin-glass (SG), and disordered (D) phases are seen. This truly unusual spin-glass phase diagram, actually does not have an antiferromagnetic phase but has a spin-glass phase. Bottom panel: Chaos inside the spin-glass phase in $d = 1$. The spin-glass phase shows the chaos under rescaling signature [13–16], in a richer version than previously: In the long-range interaction of this system, the interactions at every separation become chaotic, as seen in the lower panel of this figure, yielding a piecewise chaotic interaction potential.

regime. In this regime, a strong-coupling phase transition occurs, as shown in the next Sec. V.

To calculate the energy densities $u_{r_2-r_1} =< s_{r_1} s_{r_2} >$, the additive constant in the Hamiltonian, which always appears under renormalization-group transformation, has to be included,

$$-\beta\mathcal{H} = \sum_{r_1 \neq r_2} [J_{r_2-r_1} s_{r_1} s_{r_2} + G_{r_2-r_1}] + H \sum_{r_1} s_{r_1} , \quad (8)$$

The recursion relation of Eq. (5) has to be incremented by

$$\tilde{G}_{r'} = \frac{1}{4} \ln R_{r'}(+1,+1) R_{r'}(-1,-1) R_{r'}(+1,-1) R_{r'}(-1,+1), \quad (9)$$

where $\tilde{G}_r$ is the additive constant generated, for a given bond, by the renormalization-group transformation. For the entire system, the additive constant generated by the entire renormalization-group trajectory is

$$G = \sum_r \sum_{n=1}^{\infty} b^{-n} \tilde{G}_r^n , \quad (10)$$

where the first sum is over all pairs of spins and n designates the nth renormalization-group transformation. The energy densities are obtained by differentiating,

$$u_r = \frac{1}{N} \frac{dG}{dJ_r}, \quad (11)$$

where N is the number of spins in the original systems.

The calculated energy densities are shown in Fig. 5. Specifically, it is seen that the energy curve is smooth at the discontinuous magnetization transition at $a = 2$, which is therefore a hybrid phase transition [11], namely with a discontinuous magnetization and smooth energy curve.

V. RENORMALIZATION-GROUP THEORY OF THE EQUIVALENT-NEIGHBOR MODEL: STRONG-COUPLING PHASE TRANSITION

It seen above that the ferromagnetic phase transition temperature goes to infinity in the equivalent-neighbor region. Nevertheless, a strong-coupling phase transition [12] can be seen by scaling the interaction with the system size. In terms of $K = J/N$, at strong coupling, the renormalization-group recursion relation of Eq.(5) becomes

$$K' = 8K - uK - \ln p/2, \quad (12)$$

which has a critical (unstable) fixed point at $J = \ln p/2(7-u)$.

VI. FINITE-TEMPERATURE SPIN-GLASS PHASE IN $d = 1$ WITHOUT ANTIFERROMAGNETIC PHASE

The antiferromagnetic, overly frustrated without randomness, system does not have a finite-temperature phase transition, but the spin-glass system, where all couplings for all separations are randomly ferromagnetic or antiferromagnetic (with probability p), does have finite-temperature spin-glass phase transitions and chaos inside the spin-glass phase, as seen in Fig. 5.

The spin-glass system, where all couplings for all separations are randomly ferromagnetic or antiferromagnetic (with probability p), does have finite-temperature spin-glass phase transitions and chaos inside the spin-glass phase, as seen in Fig. 4. This truly unusual spin-glass

phase diagram, actually does not have an antiferromagnetic phase but has a spin-glass phase. Nevertheless, typical spin-glass system reentrance [**?**] is seen in this phase diagram, where as temperature is lowered at fixed antiferromagnetic bond concentration p, the ferromagnetic phase appears, but disappears at further lower temperature.

The spin-glass phase shows the chaos under rescaling signature [13–16], in a richer version than previously: In the long-range interaction of this system, the interactions at every separation become chaotic, as seen in the lower panel of Fig. 4, yielding a piecewise chaotic interaction potential.

For a previous $d = 1$ Ising spin-glass study, with short-range interactions and a zero-temperature spin-glass phase, see [17].

VII. CONCLUSION

We have solved the $d = 1$ Ising ferromagnet, antiferromagnet, and spin glass with long-range power-law interactions $J\,r^{-a}$, for all interaction range exponents a by a renormalization-group transformation that simultaneously projects local ferromagnetism, antiferromagnetism, and spin-glass order. In the ferromagnetic case, $J > 0$, a finite-temperature second-order ferromagnetic phase occurs for interaction range $0.74 < a < 2$. The second-order phase transition temperature monotonically decreases between these two limits. At $a = 2$, the phase transition becomes first order, as predicted by rigorous results. For $a > 2$, the phase transition temperature discontinuously drops to zero and for $a > 2$ there is no ordered phase above zero temperature, also as predicted by rigorous results. At the other end, on approaching $a = 0.74$ from above, namely increasing the range of the interaction, the phase transition temperature diverges to infinity, meaning that, at all non-infinite temperatures, the system is ferromagnetically ordered. Thus, the equivalent-neighbor interactions regime is entered before ($a > 0$) the neighbors become equivalent, namely before the interactions become equal ($a = 0$) for all separations. The critical exponents $\alpha, \beta, \gamma, \delta, \eta, \nu$ for the second-order phase transitions are calculated, from a large recursion matrix, varying as a function of a.

For the antiferromagnetic case, $J < 0$, all triplets of spins at all ranges have competing interactions and this highly frustrated system does not have an ordered phase.

In the spin-glass system, where all couplings for all separations are randomly ferromagnetic or antiferromagnetic (with probability p), a finite-temperatures spin-glass phase is obtained in the absence of antiferromagnetic phase. A truly unusual phase diagram, with reentrance around the ferromagnetic phase, is obtained. In the spin-glass phase, the signature chaotic behavior under scale change occurs in a richer version than previously: In the long-range interaction of this system, the interactions at every separation become chaotic, yielding a piecewise chaotic interaction function.

ACKNOWLEDGMENTS

Support by the Academy of Sciences of Turkey (TÜBA) is gratefully acknowledged.

[1] D. J. Thouless, Long-Range Order in One-Dimensional Ising Systems, Phys. Rev. **187**, 732 (1969).

[2] D. Ruelle, Statistical Mechanics Rigorous Results (Benjamin, New York, 1969).

[3] R. B. Griffiths, Rigorous Results and Theorems, in Phase Transitions and Critical Phenomena, edited by C. Domb and M. S. Green (Academic, New York, 1972), Vol. 1.

[4] M. Aizenman and C. Newman, Discontinuity of the Percolation Density in One-Dimensional $1/[X - Y]^2$ Percolation Models, Comm. Math. Phys. **107**, 611 (1986).

[5] M. Aizenman, J. Chase, L. Chase, and C. Newman, Discontunuity of the Magnetization in One-Dimensional $1/|x - y|^2$ Ising and Potts Models, J. Stat. Phys. **50**, 1 (1988).

[6] T. Niemeyer and J. M. J. van Leeuwen, Physica (Utr.) **71**, 17 (1974).

[7] J. M. J. van Leeuwen, Singularities in the Critical Surface and Universality for Ising-Like Spin Systems, Phys. Rev. Lett. **34**, 1056 (1975).

[8] A. N. Berker and M. Wortis, Blume-Emery-Griffiths-Potts Model in Two Dimensions: Phase Diagram and Critical Properties from a Position-Space Renormalization Group, Phys. Rev. B **14**, 4946 (1976).

[9] M. E. Fisher and A. N. Berker, Scaling for First-Order Phase Transitions in Thermodynamic and Finite Systems Phys. Rev. B **26** 2507 (1982).

[10] E. C. Artun and A. N. Berker, Complete Density Calculations of q-State Potts and Clock Models: Reentrance of Interface Densities under Symmetry Breaking, Phys. Rev. E **102**, 062135 (2020).

[11] S. R. McKay and A. N. Berker, Equimagnetization Lines in the Hybrid-Order Phase Diagram of the d=3 Random-Field Ising Model, J. Appl. Phys. **4**, 5785 (1988).

[12] A. N. Berker, D. Andelman, and A. Aharony, First- and Second-Order Phase Transitions of Infinite-State Potts Models in One Dimension, J. Phys. A **13**13, L413 (1980).

[13] S. R. McKay, A. N. Berker, and S. Kirkpatrick, Spin-glass behavior in frustrated Ising models with chaotic renormalization-group trajectories, Phys. Rev. Lett. **48**, 767 (1982).

[14] S. R. McKay, A. N. Berker, and S. Kirkpatrick, Amorphously packed, frustrated hierarchical models: Chaotic rescaling and spin-glass behavior, J. Appl. Phys. **53**, 7974 (1982).

[15] S. R. McKay and A. N. Berker, J. Appl. Phys., Chaotic Spin Glasses: An Upper Critical Dimension, J. Appl.

Phys. **55**, 1646 (1984).
[16] A. N. Berker and S. R. McKay, Hierarchical Models and Chaotic Spin Glasses, J. Stat. Phys. **36**, 787 (1984).
[17] G. Grinstein, A. N. Berker, J. Chalupa, and M. Wortis, Phys. Exact Renormalization Group with Griffiths Singularities and Spin-Glass Behavior: The Random Ising Chain, Phys. Rev. Lett. **50**, 1 (1988).